

Search for the $Y(4140)$ via $e^+e^- \rightarrow \gamma\phi J/\psi$ at $\sqrt{s} = 4.23, 4.26$ and 4.36 GeV

M. Ablikim¹, M. N. Achasov^{8,a}, X. C. Ai¹, O. Albayrak⁴, M. Albrecht³, D. J. Ambrose⁴³, A. Amoroso^{47A,47C}, F. F. An¹, Q. An⁴⁴, J. Z. Bai¹, R. Baldini Ferroli^{19A}, Y. Ban³⁰, D. W. Bennett¹⁸, J. V. Bennett⁴, M. Bertani^{19A}, D. Bettoni^{20A}, J. M. Bian⁴², F. Bianchi^{47A,47C}, E. Boger^{22,h}, O. Bondarenko²⁴, I. Boyko²², R. A. Briere⁴, H. Cai⁴⁹, X. Cai¹, O. Cakir^{39A,b}, A. Calcaterra^{19A}, G. F. Cao¹, S. A. Cetin^{39B}, J. F. Chang¹, G. Chelkov^{22,c}, G. Chen¹, H. S. Chen¹, H. Y. Chen², J. C. Chen¹, M. L. Chen¹, S. J. Chen²⁸, X. Chen¹, X. R. Chen²⁵, Y. B. Chen¹, H. P. Cheng¹⁶, X. K. Chu³⁰, G. Cibinetto^{20A}, D. Cronin-Hennessy⁴², H. L. Dai¹, J. P. Dai³³, A. Dbeyssi¹³, D. Dedovich²², Z. Y. Deng¹, A. Denig²¹, I. Denysenko²², M. Destefanis^{47A,47C}, F. De Mori^{47A,47C}, Y. Ding²⁶, C. Dong²⁹, J. Dong¹, L. Y. Dong¹, M. Y. Dong¹, S. X. Du⁵¹, P. F. Duan¹, J. Z. Fan³⁸, J. Fang¹, S. S. Fang¹, X. Fang⁴⁴, Y. Fang¹, L. Fava^{47B,47C}, F. Feldbauer²¹, G. Felici^{19A}, C. Q. Feng⁴⁴, E. Fioravanti^{20A}, M. Fritsch^{13,21}, C. D. Fu¹, Q. Gao¹, Y. Gao³⁸, I. Garzia^{20A}, K. Goetzen⁹, W. X. Gong¹, W. Gradl²¹, M. Greco^{47A,47C}, M. H. Gu¹, Y. T. Gu¹¹, Y. H. Guan¹, A. Q. Guo¹, L. B. Guo²⁷, T. Guo²⁷, Y. Guo¹, Y. P. Guo²¹, Z. Haddadi²⁴, A. Hafner²¹, S. Han⁴⁹, Y. L. Han¹, F. A. Harris⁴¹, K. L. He¹, Z. Y. He²⁹, T. Held³, Y. K. Heng¹, Z. L. Hou¹, C. Hu²⁷, H. M. Hu¹, J. F. Hu^{47A}, T. Hu¹, Y. Hu¹, G. M. Huang⁵, G. S. Huang⁴⁴, H. P. Huang⁴⁹, J. S. Huang¹⁴, X. T. Huang³², Y. Huang²⁸, T. Hussain⁴⁶, Q. Ji¹, Q. P. Ji²⁹, X. B. Ji¹, X. L. Ji¹, L. L. Jiang¹, L. W. Jiang⁴⁹, X. S. Jiang¹, J. B. Jiao³², Z. Jiao¹⁶, D. P. Jin¹, S. Jin¹, T. Johansson⁴⁸, A. Julin⁴², N. Kalantar-Nayestanaki²⁴, X. L. Kang¹, X. S. Kang²⁹, M. Kavatsyuk²⁴, B. C. Ke⁴, R. Kliemt¹³, B. Kloss²¹, O. B. Kolcu^{39B,d}, B. Kopf³, M. Kornicer⁴¹, W. Kuehn²³, A. Kupsc⁴⁸, W. Lai¹, J. S. Lange²³, M. Lara¹⁸, P. Larin¹³, C. H. Li¹, Cheng Li⁴⁴, D. M. Li⁵¹, F. Li¹, G. Li¹, H. B. Li¹, J. C. Li¹, Jin Li³¹, K. Li¹², K. Li³², P. R. Li⁴⁰, T. Li³², W. D. Li¹, W. G. Li¹, X. L. Li³², X. M. Li¹¹, X. N. Li¹, X. Q. Li²⁹, Z. B. Li³⁷, H. Liang⁴⁴, Y. F. Liang³⁵, Y. T. Liang²³, G. R. Liao¹⁰, D. X. Lin¹³, B. J. Liu¹, C. L. Liu⁴, C. X. Liu¹, F. H. Liu³⁴, Fang Liu¹, Feng Liu⁵, H. B. Liu¹¹, H. H. Liu¹, H. H. Liu¹⁵, H. M. Liu¹, J. Liu¹, J. P. Liu⁴⁹, J. Y. Liu¹, K. Liu³⁸, K. Y. Liu²⁶, L. D. Liu³⁰, P. L. Liu¹, Q. Liu⁴⁰, S. B. Liu⁴⁴, X. Liu²⁵, X. X. Liu⁴⁰, Y. B. Liu²⁹, Z. A. Liu¹, Zhiqiang Liu¹, Zhiqing Liu²¹, H. Loehner²⁴, X. C. Lou^{1,e}, H. J. Lu¹⁶, J. G. Lu¹, R. Q. Lu¹⁷, Y. Lu¹, Y. P. Lu¹, C. L. Luo²⁷, M. X. Luo⁵⁰, T. Luo⁴¹, X. L. Luo¹, M. Lv¹, X. R. Lyu⁴⁰, F. C. Ma²⁶, H. L. Ma¹, L. L. Ma³², Q. M. Ma¹, S. Ma¹, T. Ma¹, X. N. Ma²⁹, X. Y. Ma¹, F. E. Maas¹³, M. Maggiora^{47A,47C}, Q. A. Malik⁴⁶, Y. J. Ma³⁰, Z. P. Mao¹, S. Marcello^{47A,47C}, J. G. Messchendorp²⁴, J. Min¹, T. J. Min¹, R. E. Mitchell¹⁸, X. H. Mo¹, Y. J. Mo⁵, C. Morales Morales¹³, K. Moriya¹⁸, N. Yu. Muchnoi^{8,a}, H. Muramatsu⁴², Y. Nefedov²², F. Nerling¹³, I. B. Nikolaev^{8,a}, Z. Ning¹, S. Nisar⁷, S. L. Niu¹, X. Y. Niu¹, S. L. Olsen³¹, Q. Ouyang¹, S. Pacetti^{19B}, P. Patteri^{19A}, M. Pelizaeus³, H. P. Peng⁴⁴, K. Peters⁹, J. L. Ping²⁷, R. G. Ping¹, R. Poling⁴², Y. N. Pu¹⁷, M. Qi²⁸, S. Qian¹, C. F. Qiao⁴⁰, L. Q. Qin³², N. Qin⁴⁹, X. S. Qin¹, Y. Qin³⁰, Z. H. Qin¹, J. F. Qiu¹, K. H. Rashid⁴⁶, C. F. Redmer²¹, H. L. Ren¹⁷, M. Ripka²¹, G. Rong¹, X. D. Ruan¹¹, V. Santoro^{20A}, A. Sarantsev^{22,f}, M. Savrié^{20B}, K. Schoenning⁴⁸, S. Schumann²¹, W. Shan³⁰, M. Shao⁴⁴, C. P. Shen², P. X. Shen²⁹, X. Y. Shen¹, H. Y. Sheng¹, M. R. Shepherd¹⁸, W. M. Song¹, X. Y. Song¹, S. Sosio^{47A,47C}, S. Spataro^{47A,47C}, B. Spruck²³, G. X. Sun¹, J. F. Sun¹⁴, S. S. Sun¹, Y. J. Sun⁴⁴, Y. Z. Sun¹, Z. J. Sun¹, Z. T. Sun¹⁸, C. J. Tang³⁵, X. Tang¹, I. Tapan^{39C}, E. H. Thorndike⁴³, M. Tiemens²⁴, D. Toth⁴², M. Ullrich²³, I. Uman^{39B}, G. S. Varner⁴¹, B. Wang²⁹, B. L. Wang⁴⁰, D. Wang³⁰, D. Y. Wang³⁰, K. Wang¹, L. L. Wang¹, L. S. Wang¹, M. Wang³², P. Wang¹, P. L. Wang¹, Q. J. Wang¹, S. G. Wang³⁰, W. Wang¹, X. F. Wang³⁸, Y. D. Wang^{19A}, Y. F. Wang¹, Y. Q. Wang²¹, Z. Wang¹, Z. G. Wang¹, Z. H. Wang⁴⁴, Z. Y. Wang¹, T. Weber²¹, D. H. Wei¹⁰, J. B. Wei³⁰, P. Weidenkaff²¹, S. P. Wen¹, U. Wiedner³, M. Wolke⁴⁸, L. H. Wu¹, Z. Wu¹, L. G. Xia³⁸, Y. Xia¹⁷, D. Xiao¹, Z. J. Xiao²⁷, Y. G. Xie¹, G. F. Xu¹, L. Xu¹, Q. J. Xu¹², Q. N. Xu⁴⁰, X. P. Xu³⁶, L. Yan⁴⁴, W. B. Yan⁴⁴, W. C. Yan⁴⁴, Y. H. Yan¹⁷, H. X. Yang¹, L. Yang⁴⁹, Y. Yang⁵, Y. X. Yang¹⁰, H. Ye¹, M. Ye¹, M. H. Ye⁶, J. H. Yin¹, B. X. Yu¹, C. X. Yu²⁹, H. W. Yu³⁰, J. S. Yu²⁵, C. Z. Yuan¹, W. L. Yuan²⁸, Y. Yuan¹, A. Yuncu^{39B,g}, A. A. Zafar⁴⁶, A. Zallo^{19A}, Y. Zeng¹⁷, B. X. Zhang¹, B. Y. Zhang¹, C. Zhang²⁸, C. C. Zhang¹, D. H. Zhang³⁷, H. Y. Zhang¹, J. J. Zhang¹, J. L. Zhang¹, J. Q. Zhang¹, J. W. Zhang¹, J. Y. Zhang¹, J. Z. Zhang¹, K. Zhang¹, L. Zhang¹, S. H. Zhang¹, X. J. Zhang¹, X. Y. Zhang³², Y. Zhang¹, Y. H. Zhang¹, Z. H. Zhang⁵, Z. P. Zhang⁴⁴, Z. Y. Zhang⁴⁹, G. Zhao¹, J. W. Zhao¹, J. Y. Zhao¹, J. Z. Zhao¹, Lei Zhao⁴⁴, Ling Zhao¹, M. G. Zhao²⁹, Q. Zhao¹, Q. W. Zhao¹, S. J. Zhao⁵¹, T. C. Zhao¹, Y. B. Zhao¹, Z. G. Zhao⁴⁴, A. Zhemchugov^{22,h}, B. Zheng⁴⁵, J. P. Zheng¹, W. J. Zheng³², Y. H. Zheng⁴⁰, B. Zhong²⁷, L. Zhou¹, Li Zhou²⁹, X. Zhou⁴⁹, X. K. Zhou⁴⁴, X. R. Zhou⁴⁴, X. Y. Zhou¹, K. Zhu¹, K. J. Zhu¹, S. Zhu¹, X. L. Zhu³⁸, Y. C. Zhu⁴⁴, Y. S. Zhu¹, Z. A. Zhu¹, J. Zhuang¹, B. S. Zou¹, J. H. Zou¹

(BESIII Collaboration)

¹ Institute of High Energy Physics, Beijing 100049, People's Republic of China² Beihang University, Beijing 100191, People's Republic of China³ Bochum Ruhr-University, D-44780 Bochum, Germany⁴ Carnegie Mellon University, Pittsburgh, Pennsylvania 15213, USA⁵ Central China Normal University, Wuhan 430079, People's Republic of China⁶ China Center of Advanced Science and Technology, Beijing 100190, People's Republic of China⁷ COMSATS Institute of Information Technology, Lahore, Defence Road, Off Raiwind Road, 54000 Lahore, Pakistan⁸ G.I. Budker Institute of Nuclear Physics SB RAS (BINP), Novosibirsk 630090, Russia⁹ GSI Helmholtzcentre for Heavy Ion Research GmbH, D-64291 Darmstadt, Germany¹⁰ Guangxi Normal University, Guilin 541004, People's Republic of China¹¹ GuangXi University, Nanning 530004, People's Republic of China¹² Hangzhou Normal University, Hangzhou 310036, People's Republic of China¹³ Helmholtz Institute Mainz, Johann-Joachim-Becher-Weg 45, D-55099 Mainz, Germany¹⁴ Henan Normal University, Xinxiang 453007, People's Republic of China¹⁵ Henan University of Science and Technology, Luoyang 471003, People's Republic of China¹⁶ Huangshan College, Huangshan 245000, People's Republic of China¹⁷ Hunan University, Changsha 410082, People's Republic of China

- ¹⁸ Indiana University, Bloomington, Indiana 47405, USA
- ¹⁹ (A)INFN Laboratori Nazionali di Frascati, I-00044, Frascati, Italy; (B)INFN and University of Perugia, I-06100, Perugia, Italy
- ²⁰ (A)INFN Sezione di Ferrara, I-44122, Ferrara, Italy; (B)University of Ferrara, I-44122, Ferrara, Italy
- ²¹ Johannes Gutenberg University of Mainz, Johann-Joachim-Becher-Weg 45, D-55099 Mainz, Germany
- ²² Joint Institute for Nuclear Research, 141980 Dubna, Moscow region, Russia
- ²³ Justus Liebig University Giessen, II. Physikalisches Institut, Heinrich-Buff-Ring 16, D-35392 Giessen, Germany
- ²⁴ KVI-CART, University of Groningen, NL-9747 AA Groningen, The Netherlands
- ²⁵ Lanzhou University, Lanzhou 730000, People's Republic of China
- ²⁶ Liaoning University, Shenyang 110036, People's Republic of China
- ²⁷ Nanjing Normal University, Nanjing 210023, People's Republic of China
- ²⁸ Nanjing University, Nanjing 210093, People's Republic of China
- ²⁹ Nankai University, Tianjin 300071, People's Republic of China
- ³⁰ Peking University, Beijing 100871, People's Republic of China
- ³¹ Seoul National University, Seoul, 151-747 Korea
- ³² Shandong University, Jinan 250100, People's Republic of China
- ³³ Shanghai Jiao Tong University, Shanghai 200240, People's Republic of China
- ³⁴ Shanxi University, Taiyuan 030006, People's Republic of China
- ³⁵ Sichuan University, Chengdu 610064, People's Republic of China
- ³⁶ Soochow University, Suzhou 215006, People's Republic of China
- ³⁷ Sun Yat-Sen University, Guangzhou 510275, People's Republic of China
- ³⁸ Tsinghua University, Beijing 100084, People's Republic of China
- ³⁹ (A)Istanbul Aydin University, 34295 Sefakoy, Istanbul, Turkey; (B)Dogus University, 34722 Istanbul, Turkey; (C)Uludag University, 16059 Bursa, Turkey
- ⁴⁰ University of Chinese Academy of Sciences, Beijing 100049, People's Republic of China
- ⁴¹ University of Hawaii, Honolulu, Hawaii 96822, USA
- ⁴² University of Minnesota, Minneapolis, Minnesota 55455, USA
- ⁴³ University of Rochester, Rochester, New York 14627, USA
- ⁴⁴ University of Science and Technology of China, Hefei 230026, People's Republic of China
- ⁴⁵ University of South China, Hengyang 421001, People's Republic of China
- ⁴⁶ University of the Punjab, Lahore-54590, Pakistan
- ⁴⁷ (A)University of Turin, I-10125, Turin, Italy; (B)University of Eastern Piedmont, I-15121, Alessandria, Italy; (C)INFN, I-10125, Turin, Italy
- ⁴⁸ Uppsala University, Box 516, SE-75120 Uppsala, Sweden
- ⁴⁹ Wuhan University, Wuhan 430072, People's Republic of China
- ⁵⁰ Zhejiang University, Hangzhou 310027, People's Republic of China
- ⁵¹ Zhengzhou University, Zhengzhou 450001, People's Republic of China
- ^a Also at the Novosibirsk State University, Novosibirsk, 630090, Russia
- ^b Also at Ankara University, 06100 Tandogan, Ankara, Turkey
- ^c Also at the Moscow Institute of Physics and Technology, Moscow 141700, Russia and at the Functional Electronics Laboratory, Tomsk State University, Tomsk, 634050, Russia
- ^d Currently at Istanbul Arel University, Kucukcekmece, Istanbul, Turkey
- ^e Also at University of Texas at Dallas, Richardson, Texas 75083, USA
- ^f Also at the PNPI, Gatchina 188300, Russia
- ^g Also at Bogazici University, 34342 Istanbul, Turkey
- ^h Also at the Moscow Institute of Physics and Technology, Moscow 141700, Russia

(Dated: August 27, 2018)

Using data samples collected at center-of-mass energies $\sqrt{s} = 4.23, 4.26, \text{ and } 4.36$ GeV with the BESIII detector operating at the BEPCII storage ring, we search for the production of the charmoniumlike state $Y(4140)$ through a radiative transition followed by its decay to $\phi J/\psi$. No significant signal is observed and upper limits on $\sigma[e^+e^- \rightarrow \gamma Y(4140)] \cdot \mathcal{B}(Y(4140) \rightarrow \phi J/\psi)$ at the 90% confidence level are estimated as 0.35, 0.28, and 0.33 pb at $\sqrt{s} = 4.23, 4.26, \text{ and } 4.36$ GeV, respectively.

PACS numbers: 14.40.Rt, 13.66.Bc, 14.40.Pq, 13.20.Gd

I. INTRODUCTION

The CDF experiment first reported evidence for a new state called $Y(4140)$ in the decay $B^+ \rightarrow \phi J/\psi K^+$ [1]. In a subse-

quent analysis, CDF claimed the observation of the $Y(4140)$ with a statistical significance greater than 5σ with a mass of $[4143.4_{-3.0}^{+2.9}(\text{stat}) \pm 0.6(\text{syst})]$ MeV/ c^2 and a width of

[$15.3_{-0.1}^{+10.4}(\text{stat}) \pm 2.5(\text{syst})$] MeV [2]. However, the existence of the $Y(4140)$ was not confirmed by the Belle [3] or LHCb [4] collaborations in the same process, nor by the Belle collaboration in two-photon production [3]. Recently, the CMS [5] and D0 [6] collaborations reported on analyses of $B^+ \rightarrow \phi J/\psi K^+$, where an accumulation of events is observed in the $\phi J/\psi$ invariant mass distribution, with resonance parameters consistent with those of the CDF measurement. The BABAR collaboration also investigated the same decay mode, and found no evidence for the $Y(4140)$ [7].

Being well above the open charm threshold, the narrow structure $Y(4140)$ is difficult to be interpreted as a conventional charmonium state [8], while it is a good candidate for a molecular [9–14], $c\bar{c}s\bar{s}$ tetraquark [15], or charmonium hybrid state [10]. A detailed review on the $Y(4140)$ is given in Ref. [16]. The $Y(4140)$ is the first charmoniumlike state decaying into two vector mesons consisting of $c\bar{c}$ and $s\bar{s}$ pairs. Since both the ϕ and J/ψ have $J^{PC} = 1^{--}$, the $\phi J/\psi$ system has positive C-parity, and can be searched for through radiative transitions of $Y(4260)$ or other 1^{--} charmonium or charmoniumlike states. The author of Ref. [10] found that the partial width of the radiative transition $Y(4260) \rightarrow \gamma Y(4140)$ may be up to several tens of keV if both the $Y(4260)$ and $Y(4140)$ are hybrid charmonium states. The data samples collected at center-of-mass (CM) energies near the $Y(4260)$ at the BESIII experiment can be used to search for such transitions.

The structure of this paper is as follows. In Sec. II, the setup for the BESIII experiment and details of the data samples are given. In Sec. III, event selections for $\phi J/\psi$ events are described for three different decay modes of the ϕ meson. Section IV details the upper limit calculations for the production of $Y(4140)$, while Sec. V describes the systematic errors of the measurement. A short summary of the results is given in Sec. VI.

II. DATA AND MONTE CARLO SAMPLES

In this paper, we present results of a search for $Y(4140)$ decays into $\phi J/\psi$ through the process $e^+e^- \rightarrow \gamma \phi J/\psi$ with data taken at CM energies of $\sqrt{s} = 4.23, 4.26, \text{ and } 4.36$ GeV. The data samples were collected with the BESIII detector operating at the BEPCII storage ring [17]. The integrated luminosity of these data samples are measured by using large-angle Bhabha scattering with an uncertainty of 1.0% [18]. The luminosities of the data samples are 1094, 827, and 545 pb^{-1} , for $\sqrt{s} = 4.23, 4.26, \text{ and } 4.36$ GeV, respectively.

The BESIII detector, described in detail in Ref. [17], has a geometrical acceptance of 93% of 4π . A small-cell helium-based main drift chamber (MDC) provides a charged particle momentum resolution of 0.5% at 1 GeV/c in a 1 T magnetic field, and supplies energy loss (dE/dx) measurements with a resolution better than 6% for electrons from Bhabha scatter-

ing. The electromagnetic calorimeter (EMC) measures photon energies with a resolution of 2.5% (5%) at 1.0 GeV in the barrel (endcaps). Particle identification (PID) is provided by a time-of-flight system (TOF) with a time resolution of 80 ps (110 ps) for the barrel (endcaps). The muon system, located in the iron flux return yoke of the magnet, provides 2 cm position resolution and detects muon tracks with momentum greater than 0.5 GeV/c.

The GEANT4-based [19] Monte Carlo (MC) simulation software BOOST [20] includes the geometric description of the BESIII detector and a simulation of the detector response. It is used to optimize event selection criteria, estimate backgrounds and evaluate the detection efficiency. For each energy point, we generate signal MC samples of $e^+e^- \rightarrow \gamma Y(4140)$, $Y(4140) \rightarrow \phi J/\psi$ uniformly in phase space, where the ϕ decays to $K^+K^-/K_S^0K_L^0/\pi^+\pi^-\pi^0$ and the J/ψ decays to $e^+e^-/\mu^+\mu^-$. The decays of $\phi \rightarrow K^+K^-$ and $K_S^0K_L^0$ are modeled as a vector particle decaying to two pseudoscalars (EVTGEN [24] model VSS), and the decay $\phi \rightarrow \rho\pi$ is modeled as a vector particle decaying to a vector and a scalar (VVS_PWAVE model), and all the other processes are generated uniformly in phase space. Effects of initial state radiation (ISR) are simulated with KKMC [21], where the Born cross section of $e^+e^- \rightarrow \gamma Y(4140)$ is assumed to follow the $Y(4260) \rightarrow \pi^+\pi^- J/\psi$ line shape [22]. Final state radiation (FSR) effects associated with charged particles are handled with PHOTOS [23].

To study possible background contributions, MC samples of inclusive $Y(4260)$ decays, equivalent to the integrated luminosity of data, are also generated at $\sqrt{s} = 4.23, 4.26$ and 4.36 GeV. In these simulations the $Y(4260)$ is allowed to decay generically, with the main known decay channels being generated using EVTGEN with branching fractions set to world average values [22]. The remaining events associated with charmonium decays are generated with LUNDCHARM [25] while continuum hadronic events are generated with PYTHIA [26]. QED events such as Bhabha, dimuon and digamma are generated with KKMC [21].

III. EVENT SELECTION

For each charged particle track, the polar angle in the MDC must satisfy $|\cos\theta| < 0.93$, and the point of closest approach to the e^+e^- interaction point (IP) must be within ± 10 cm in the beam direction and within ± 1 cm in the plane perpendicular to the beam direction, except for the $\pi^+\pi^-$ pair from K_S^0 decays. Since leptons from the J/ψ decays are kinematically well separated from other charged tracks, tracks with momenta larger than 1.0 GeV/c in the laboratory frame are assumed to be leptons. We use the energy deposited in the EMC to separate electrons from muons. For muon candidates, the deposited energy is less than 0.4 GeV, while for electrons it is larger than 1.0 GeV. EMC showers identified as photon candidates must satisfy the following requirements. The

minimum required energy deposited in the EMC is 25 MeV for the barrel ($|\cos\theta| < 0.8$) and 50 MeV for the endcaps ($0.86 < |\cos\theta| < 0.92$). To eliminate showers associated with charged particles, e.g. from bremsstrahlung, a photon must be separated by at least 20 degrees from any charged track. The timing information from the EMC is also required to be in 0-700 ns to suppress electronic noise and energy deposits unrelated to signal events.

A. $\phi \rightarrow K^+K^-$

For the $\phi \rightarrow K^+K^-$ decay mode, the momenta of the kaons are about 0.2 GeV/c in the laboratory frame. The detection efficiency for low momentum kaons is very small. In order to increase the efficiency, only one kaon is required to be found and to pass through the PID selection using both dE/dx and TOF information. To improve the mass resolution and suppress backgrounds, a one-constraint (1C) kinematic fit is performed with the $\gamma K^+K^- \ell^+ \ell^-$ ($\ell = e$ or μ) hypothesis, constraining the missing mass to the Kaon mass, and the χ^2 is required to be less than 25. This value is determined by maximizing the figure of merit (FOM) $S/\sqrt{S+B}$, where S refers to the number of signal events from the signal MC simulation and B is the number of background events from the inclusive MC sample. For the signal cross section, we use the upper limit determined in this analysis as input. The χ^2 requirement depends weakly on the cross section of signal. If there are two kaons or more than one good photon candidate, the combination with the smallest χ^2 is retained.

After imposing the requirements above, we use mass windows around the J/ψ and ϕ to select signal events. The mass windows are defined as $[\mu - W, \mu + W]$, where μ and W are the mean value and full width at half maximum (FWHM) of the invariant mass distributions of signal events from the MC simulation. The values of μ and W for each of the different decay modes of the ϕ meson considered in this analysis are listed in Table I. Figure 1 shows the scatter plots of $M(K^+K^-)$ vs. $M(\ell^+\ell^-)$ for MC and data at 4.26 GeV and the 1-D projections. No significant $\gamma\phi J/\psi$ signal is observed. The dominant background events are $e^+e^- \rightarrow K^+K^- J/\psi$ with a random photon candidate from beam related background cluster, so the mass of J/ψ is shifted by about 30 MeV/c² to the lower side. About 0.4% of these events will leak into the J/ψ mass window, but in the $M(\phi J/\psi)$ distribution, they accumulate at about 30 MeV/c² below the CM energy, far away from the nominal mass of the $Y(4140)$.

The invariant mass distributions of the $\phi J/\psi$ candidates after all event selection criteria have been applied are shown in Fig. 2, for the three data samples and the sum of them. Here we use $M(\phi J/\psi) = M(K^+K^- \ell^+ \ell^-) - M(\ell^+ \ell^-) + m_{J/\psi}$ to partially cancel the mass resolution of the lepton pair, where $m_{J/\psi}$ is the nominal mass of the J/ψ [22].

There are no events left from the inclusive MC sam-

TABLE I. The mean (μ) and FWHM (W) of the J/ψ and ϕ mass distributions, and the mass windows of the J/ψ and ϕ signals. All values are in units of MeV/c².

mode	$\mu(J/\psi)$	$W(J/\psi)$	Mass window
$\phi \rightarrow K^+K^-$	3098.9 ± 0.1	19.8 ± 0.1	3079-3119
$\phi \rightarrow K_S^0 K_L^0$	3099.1 ± 0.1	20.5 ± 0.1	3078-3120
$\phi \rightarrow \pi^+ \pi^- \pi^0$	3101.1 ± 0.1	18.6 ± 0.1	3082-3120
mode	$\mu(\phi)$	$W(\phi)$	Mass window
$\phi \rightarrow K^+K^-$	1020.1 ± 0.1	15.1 ± 0.1	1005-1036
$\phi \rightarrow K_S^0 K_L^0$	1019.8 ± 0.1	13.9 ± 0.1	1005-1034
$\phi \rightarrow \pi^+ \pi^- \pi^0$	1019.1 ± 0.1	16.8 ± 0.1	1002-1036

ple after applying all of the above selections. Since there are two high momentum leptons in the final state and the BESIII PID can separate the low momentum kaon from other particles very well, the possible backgrounds must have a K^+K^- pair and two high-momentum charged tracks. Exclusive MC samples of the processes $e^+e^- \rightarrow K^+K^- J/\psi$, $K^+K^- \pi^+ \pi^-$, $K^+K^- \pi^+ \pi^- \pi^0$ and $\phi \pi^+ \pi^-$ are generated and analyzed with more than 100,000 events each (corresponding to a cross section of 200 pb), and we confirm that no events are selected as the $Y(4140)$ signal. The cross sections of these final states have been measured to be of a few or a few tens of pb level [27–29, 31] in the energy range of interest. Backgrounds due to one photon from π^0 or η decays being misidentified as the radiative photon were checked for in the inclusive MC sample and found to be negligible.

Three-body process $e^+e^- \rightarrow \gamma\phi J/\psi$ and four-body process $\gamma K^+K^- J/\psi$ are studied with MC simulation. Even though the cross sections of these non-resonant channels are expected to be small, we cannot rule out the possibility that the three events observed in the $Y(4140)$ signal region (as shown in Fig. 2) are from non-resonant processes.

B. $\phi \rightarrow K_S^0 K_L^0$

For the $\phi \rightarrow K_S^0 K_L^0$ mode, the K_S^0 is reconstructed with its decay to $\pi^+ \pi^-$. The pions from the decay of K_S^0 can also be kinematically well separated from the leptons, and charged tracks with momenta less than 0.6 GeV/c in the laboratory frame are assumed to be pions. Since the K_S^0 has a relatively long lifetime, it travels a measurable distance before it decays. We perform a secondary vertex fit on the two charged pions to improve the mass resolution, but no extra χ^2 requirement is applied. The fitted mass and FWHM of the $\pi^+ \pi^-$ invariant mass spectrum is determined from the simulation to be $\mu = (497.6 \pm 0.1)$ MeV/c² and $W = (3.3 \pm 0.1)$ MeV/c², respectively, and we select candidates in the mass range $[\mu - W, \mu + W]$. Since the K_L^0 is difficult to be detected at BESIII, we only require that there are two pions

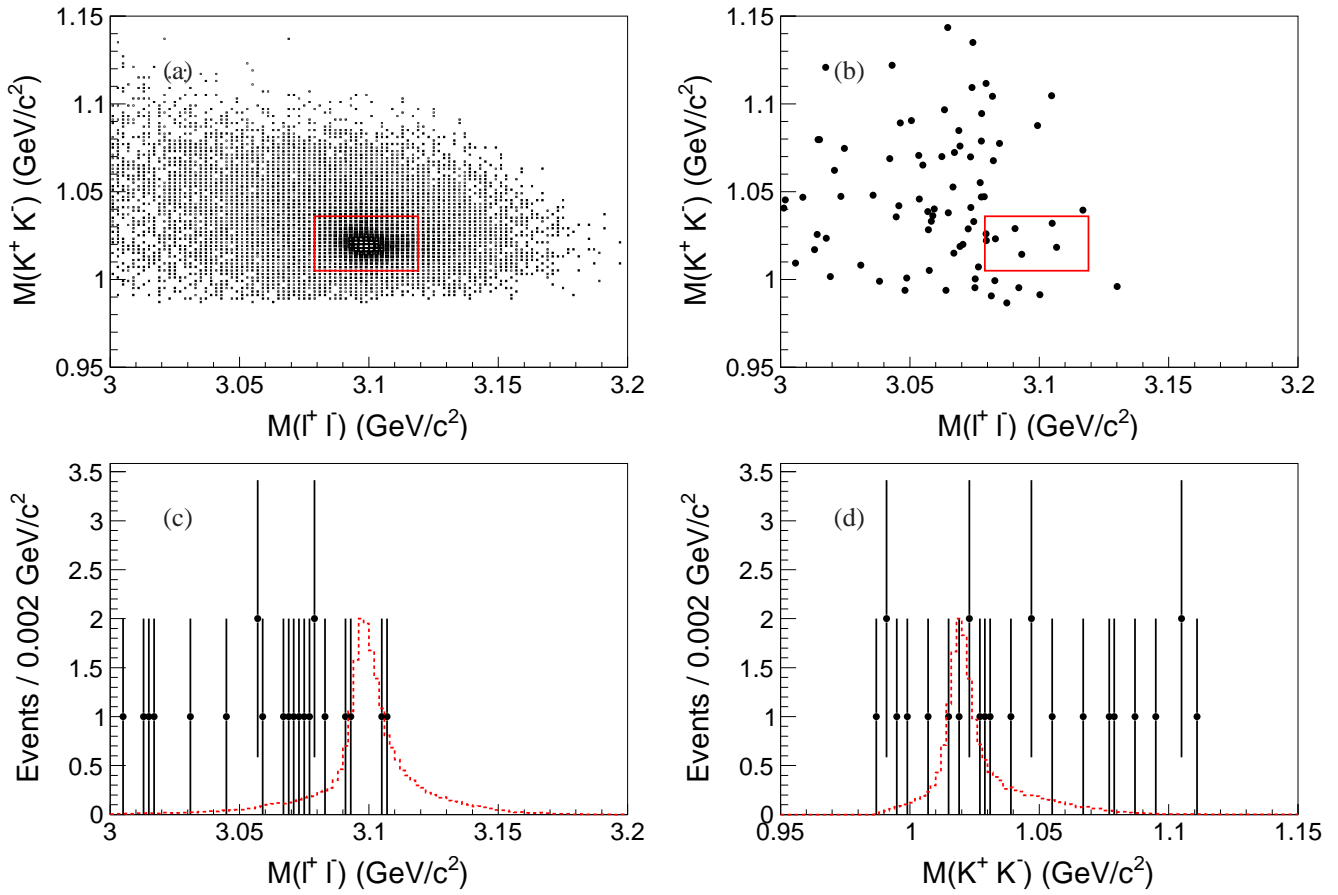


FIG. 1. Scatter plots for (a) signal MC, (b) data at 4.26 GeV and (c) the projections along $M(\ell^+\ell^-)$ in ϕ mass window and (d) the projections along $M(K^+K^-)$ in J/ψ mass window. Red box shows mass windows of ϕ and J/ψ . Red dashed histogram shows the MC simulated shape (not normalized).

and two leptons in the final state. Then the event is kinematically fitted to the hypothesis $\gamma K_S^0 K_L^0 \ell^+ \ell^-$, with the missing mass constrained to the nominal K_L^0 mass [22]. If there is more than one good photon candidate, the combination with the smallest χ^2 is used, and the χ^2 is required to be less than 20.

The mass windows around the J/ψ and ϕ used to select signal events are given in Table I. Figure 3 shows the scatter plots of $M(K_S^0 K_L^0)$ vs. $M(\ell^+ \ell^-)$ for MC and data at 4.26 GeV and the 1-D projections. The dominant background events are from $e^+ e^- \rightarrow K_S^0 K_L^0 J/\psi$ with a random photon candidate, so the mass of J/ψ is shifted too, as in the $\phi \rightarrow K^+ K^-$ mode.

To study possible backgrounds, we use the inclusive MC sample, as well as exclusive MC samples of $e^+ e^- \rightarrow K_S^0 K_L^0 J/\psi, \eta \eta J/\psi, \eta J/\psi$ and $\phi \pi^+ \pi^-$. No events survive in the $Y(4140)$ signal region. The size of each exclusive MC samples corresponds to a production cross section of 200 pb, which is larger than at least a factor of 4 of the experimental measurements [27, 28, 30, 31]. Figure 4 shows the distribution of $M(\phi J/\psi) = M(K_S^0 K_L^0 \ell^+ \ell^-) - M(\ell^+ \ell^-) + m_{J/\psi}$

after all the event selection criteria have been applied, with no obvious $Y(4140)$ or other signals. There are only 5 events in the sum of three data samples, and none of them is near the mass of the $Y(4140)$.

C. $\phi \rightarrow \pi^+ \pi^- \pi^0$

For the $\phi \rightarrow \pi^+ \pi^- \pi^0$ decay mode, the charged pions from the ϕ decays have lower momenta than the leptons from the J/ψ decay, so all charged tracks with momentum less than 0.6 GeV/c are taken to be pions. We require that there are at least three good photons in the EMC, and loop over all the combinations to select three photons with the smallest χ^2 of a four-constraint (4C) kinematic fit, which constrains the four-momenta of all particles in the final state to be that of the initial $e^+ e^-$ system. The χ^2 is required to be less than 40. We use two photons out of the three to reconstruct a π^0 candidate, whose invariant mass is nearest to the nominal mass of the π^0 [22]. The fitted mass and FWHM of the π^0 of signal events from MC simulation are $\mu = (134.1 \pm 0.1) \text{ MeV}/c^2$ and $W =$

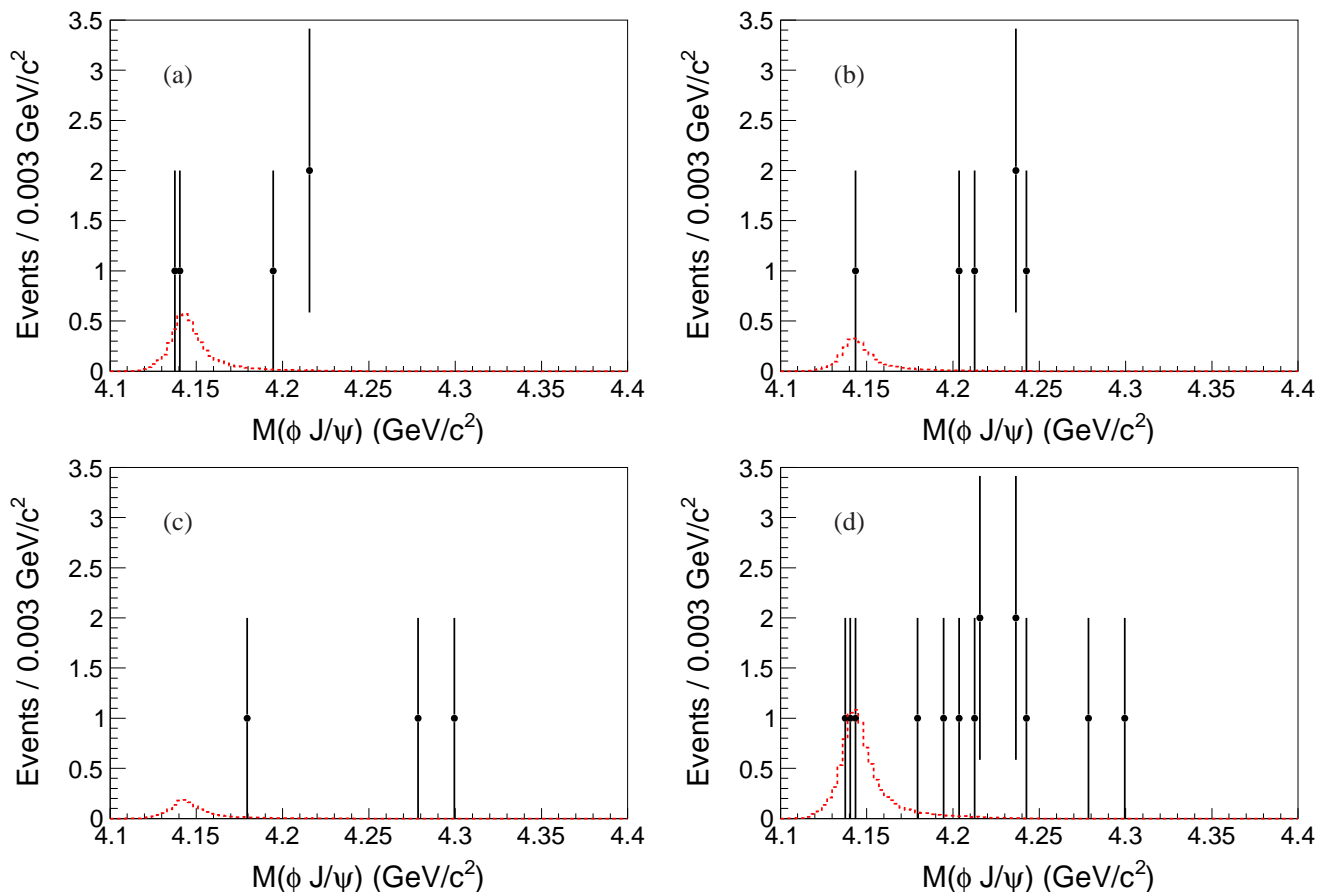


FIG. 2. Distribution of $M(\phi J/\psi)$ with ϕ decays to K^+K^- from data collected at (a) 4.23, (b) 4.26, (c) 4.36 GeV and (d) the sum of three data samples. The red dashed histograms represent signal MC samples scaled to the measured upper limits.

$(8.2 \pm 0.1) \text{ MeV}/c^2$, respectively. We select π^0 candidates in the mass range $[\mu - W, \mu + W]$, and the mass windows of J/ψ and ϕ from this mode are also shown in Table I.

Figure 5 shows the scatter plots of $M(\pi^+\pi^-\pi^0)$ vs. $M(\ell^+\ell^-)$ for MC and data at 4.26 GeV and the 1-D projections. The dominant background events are from $e^+e^- \rightarrow \omega\chi_{cJ}$ and $e^+e^- \rightarrow \eta J/\psi$ with a random photon. Neither of these channels can be selected as $\gamma\phi J/\psi$ signal.

From the inclusive MC sample and exclusive $e^+e^- \rightarrow \pi^+\pi^-\pi^0 J/\psi$ and $\eta J/\psi$ MC samples, correspond to production cross section of 200 pb, we find no events in the $Y(4140)$ signal region, so these background channels are neglected. The production cross section of the above two modes are at a few or a few tens of pb level [30, 31]. After the event selection, there are no events left for the data samples at $\sqrt{s} = 4.23$ and 4.26 GeV, and there are only two events left for the data sample at 4.36 GeV. Figure 6 shows the distribution of $M(\phi J/\psi) = M(\pi^+\pi^-\pi^0\ell^+\ell^-) - M(\ell^+\ell^-) + m_{J/\psi}$ at $\sqrt{s} = 4.36$ GeV. Both surviving events are far from the $Y(4140)$ signal region.

IV. CROSS SECTIONS

As the $Y(4140)$ signal is not significant, and it cannot be distinguished from the contribution of the non-resonant processes due to low statistics, we set an upper limit on this production rate at the 90% confidence level (C.L.). The six decay modes (three ϕ modes \times two J/ψ modes) are combined to obtain the best estimate of the $Y(4140)$ production cross section by counting the numbers of events located in the $Y(4140)$ signal region. This signal region is defined as $M(\phi J/\psi) \in [4.11, 4.17] \text{ GeV}/c^2$, which covers about 95% of the signal events according to the MC simulation. The combined distributions of $M(\phi J/\psi)$ are shown in Fig. 7. From MC studies of the known possible background channels, which are detailed in Sec. III for the three ϕ decay modes separately, no events in the signal region are observed. Since information on possible backgrounds is limited, we conservatively assume that all the events that lie in the signal region are from the $Y(4140)$. We assume that the number of observed events follows Poisson distributions. The total likelihood of the six modes is defined

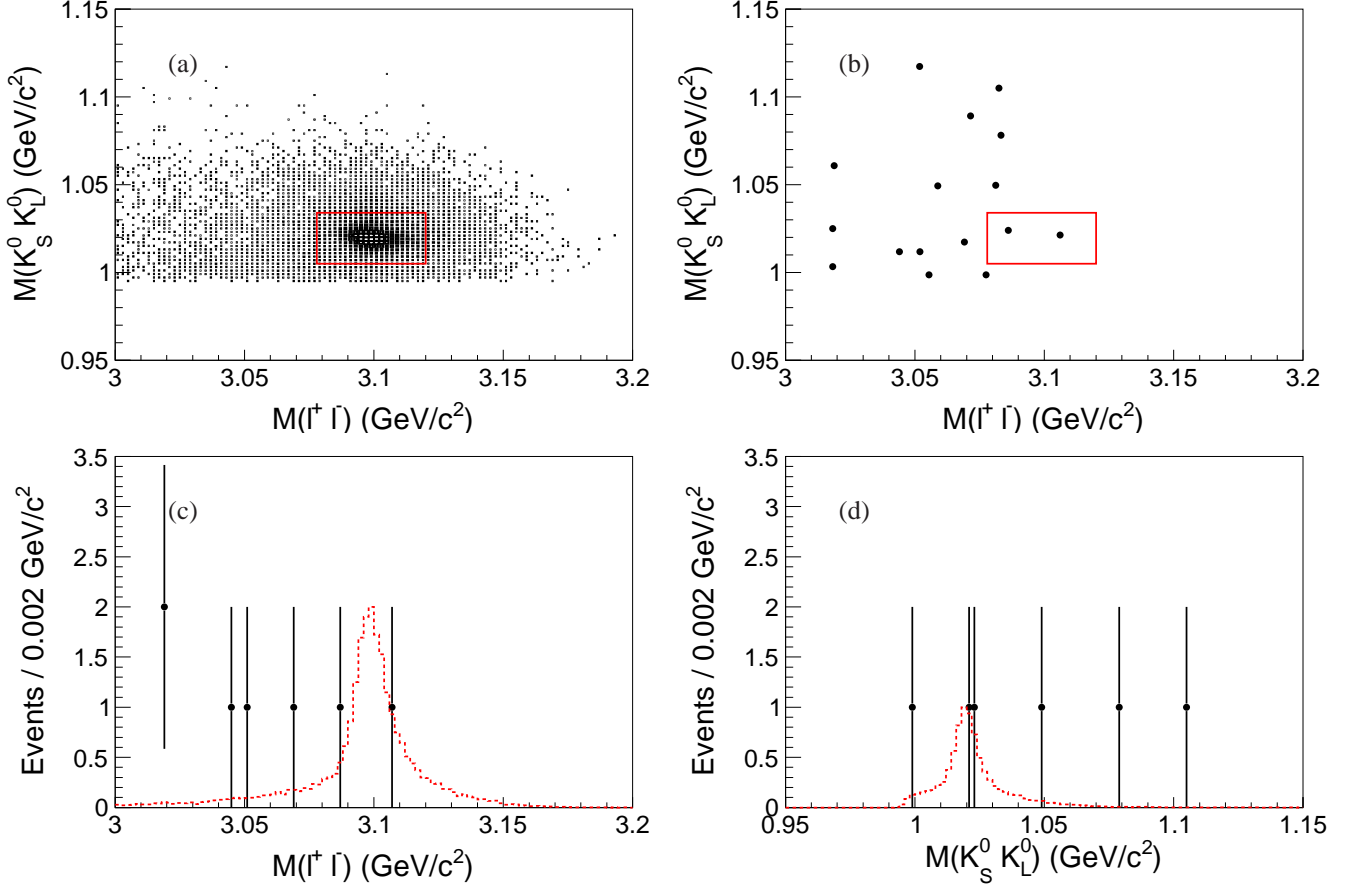


FIG. 3. Scatter plots for (a) signal MC, (b) data at 4.26 GeV and (c) the projections along $M(\ell^+\ell^-)$ in the ϕ mass window, and (d) the projections along $M(K_S^0 K_L^0)$ in the J/ψ mass window. The red box shows the mass regions used for ϕ and J/ψ . The red dashed histograms show the MC simulated shape (with arbitrary normalization).

as

$$L(n^{\text{prod}}) = \prod_{i=1}^6 P(N_i^{\text{obs}}; n^{\text{prod}} \mathcal{B}_i \epsilon_i). \quad (1)$$

Here $P(r; \mu) = \frac{1}{r!} \mu^r e^{-\mu}$ is the probability density function of a Poisson distribution, n^{prod} is the number of produced $Y(4140) \rightarrow \phi J/\psi$ events, N_i^{obs} is the number of observed events in the i th mode, \mathcal{B}_i and ϵ_i are the corresponding branching fraction and efficiency, respectively. To take systematic uncertainties into consideration, we convolute the likelihood distribution with a Gaussian function with mean value of 0 and standard deviation $n^{\text{prod}} \cdot \Delta$, where Δ is the relative systematic uncertainty described in the next section. The upper limit on n^{prod} at the 90% C.L. is obtained from $\int_0^{n^{\text{prod}}} L(x) dx / \int_0^{\infty} L(x) dx = 0.9$.

The Born cross section is calculated using

$$\sigma^B = \frac{n^{\text{prod}}}{\mathcal{L}_{\text{int}}(1 + \delta)(1 + \delta^{\text{vac}})}, \quad (2)$$

where \mathcal{L}_{int} is the integrated luminosity, $(1 + \delta)$ is the radiative

correction factor, including initial state radiation, e^+e^- self-energy and initial vertex correction, and $(1 + \delta^{\text{vac}})$ is the vacuum polarization factor, including leptonic and hadronic parts.

The radiative correction factor $(1 + \delta)$ is obtained by using a QED calculation [32]. We assume that the cross section for $e^+e^- \rightarrow \gamma Y(4140)$ follows the $Y(4260) \rightarrow \pi^+\pi^- J/\psi$ line shape, and use the Breit-Wigner parameters of the $Y(4260)$ [22] as input. The values for $(1 + \delta)$ are listed in Table II. The vacuum polarization factor $(1 + \delta^{\text{vac}}) = 1.054$ is taken from Ref. [33], and its uncertainty in comparison with other uncertainties is negligible.

The upper limit on σ^B is obtained by replacing n^{prod} with the upper limit on n^{prod} . The upper limits on the product of the Born cross section and branching fraction $\sigma[e^+e^- \rightarrow \gamma Y(4140)] \cdot \mathcal{B}(Y(4140) \rightarrow \phi J/\psi)$ at the 90% C.L. are 0.35, 0.28 and 0.33 pb for $\sqrt{s} = 4.23, 4.26$ and 4.36 GeV, respectively. The results are listed in Table II.

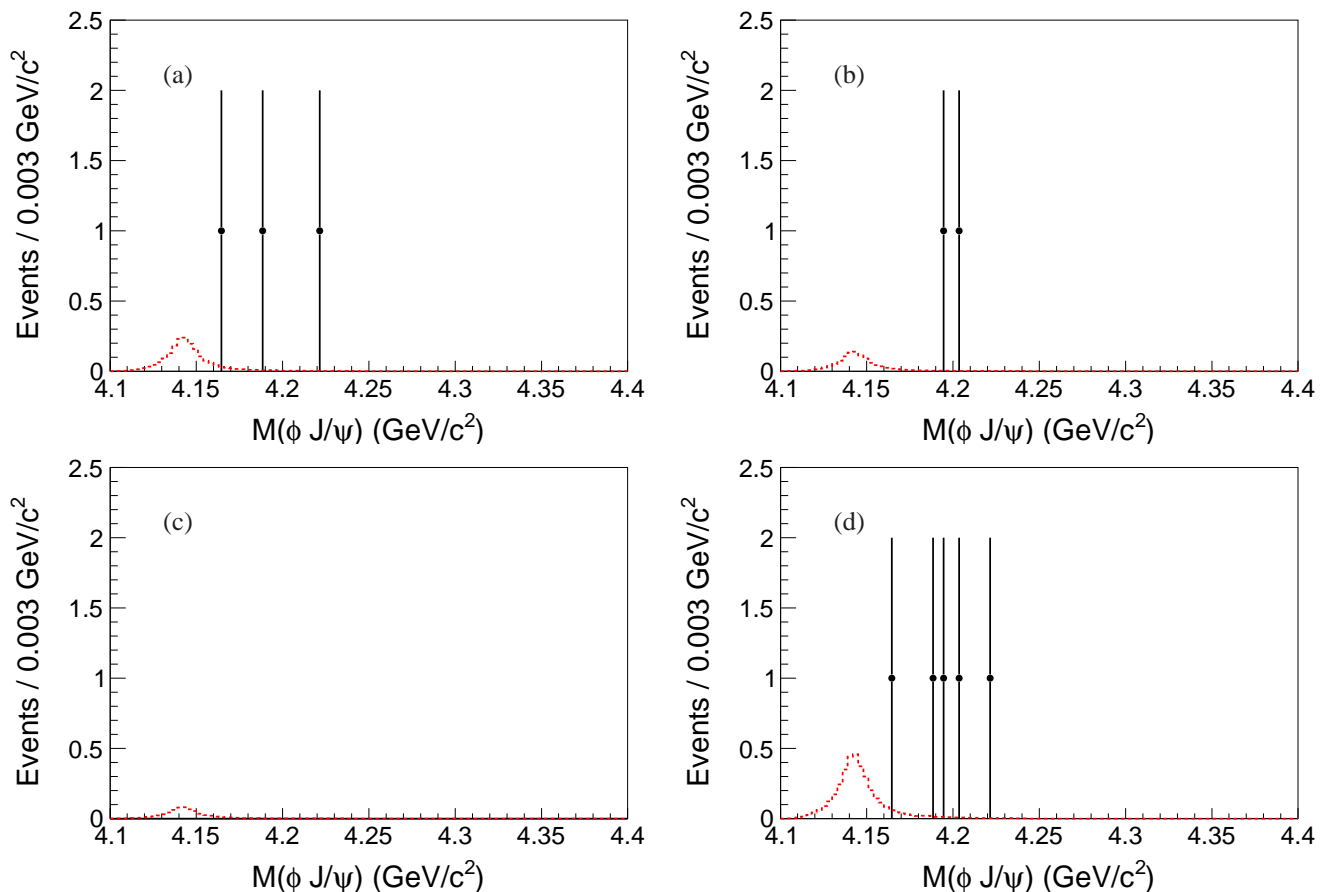


FIG. 4. Distribution of $M(\phi J/\psi)$ with ϕ decays to $K_S^0 K_L^0$ from data collected at (a) 4.23, (b) 4.26, (c) 4.36 GeV, and (d) the sum of the three data samples. The red dashed histograms represent signal MC samples which have been scaled to the measured upper limits.

TABLE II. Upper limits at the 90% C.L. for measurements of $\sigma^B \cdot \mathcal{B} = \sigma(e^+e^- \rightarrow \gamma Y(4140)) \cdot \mathcal{B}(Y(4140) \rightarrow \phi J/\psi)$.

\sqrt{s} (GeV)	Luminosity (pb^{-1})	$(1 + \delta)$	n^{prod}	$\sigma^B \cdot \mathcal{B}$ (pb)
4.23	1094	0.840	< 339	< 0.35
4.26	827	0.847	< 207	< 0.28
4.36	545	0.944	< 179	< 0.33

V. SYSTEMATIC UNCERTAINTIES

The sources of the systematic uncertainties are listed in Table III for the measurement at 4.26 GeV and are explained below.

The luminosity is measured using Bhabha events, with an uncertainty less than 1.0% [34]. The difference between data and MC in tracking efficiencies for charged tracks is 1.0% per track [35]. Studies with a sample of $J/\psi \rightarrow \rho\pi$ events show that the uncertainty in the reconstruction efficiency for photons is less than 1.0% [36]. For the $\phi \rightarrow K^+K^-$ mode,

TABLE III. Summary of systematic uncertainties for $\sqrt{s}=4.26$ GeV data sample.

Source	Systematic uncertainty (%)		
	$\phi \rightarrow K^+K^-$	$K_S^0 K_L^0$	$\pi^+\pi^-\pi^0$
Luminosity	1.0	1.0	1.0
Tracking	3.0	2.0	4.0
Photon	1.0	1.0	3.0
PID	1.0	-	-
K_S^0 reconstruction	-	4.0	-
Branching fraction	1.2	1.3	2.2
Radiative correction	3.8	3.8	3.8
Radiative decay distribution	11.5	8.8	13.5
Kinematic fit	3.8	6.4	3.2
Total	13.2	12.5	15.4

PID is required for the kaons, and this is taken as 1.0% [35] per track. Since we require only one kaon to be identified, the uncertainty is smaller than 1.0%, but we take 1.0% to be

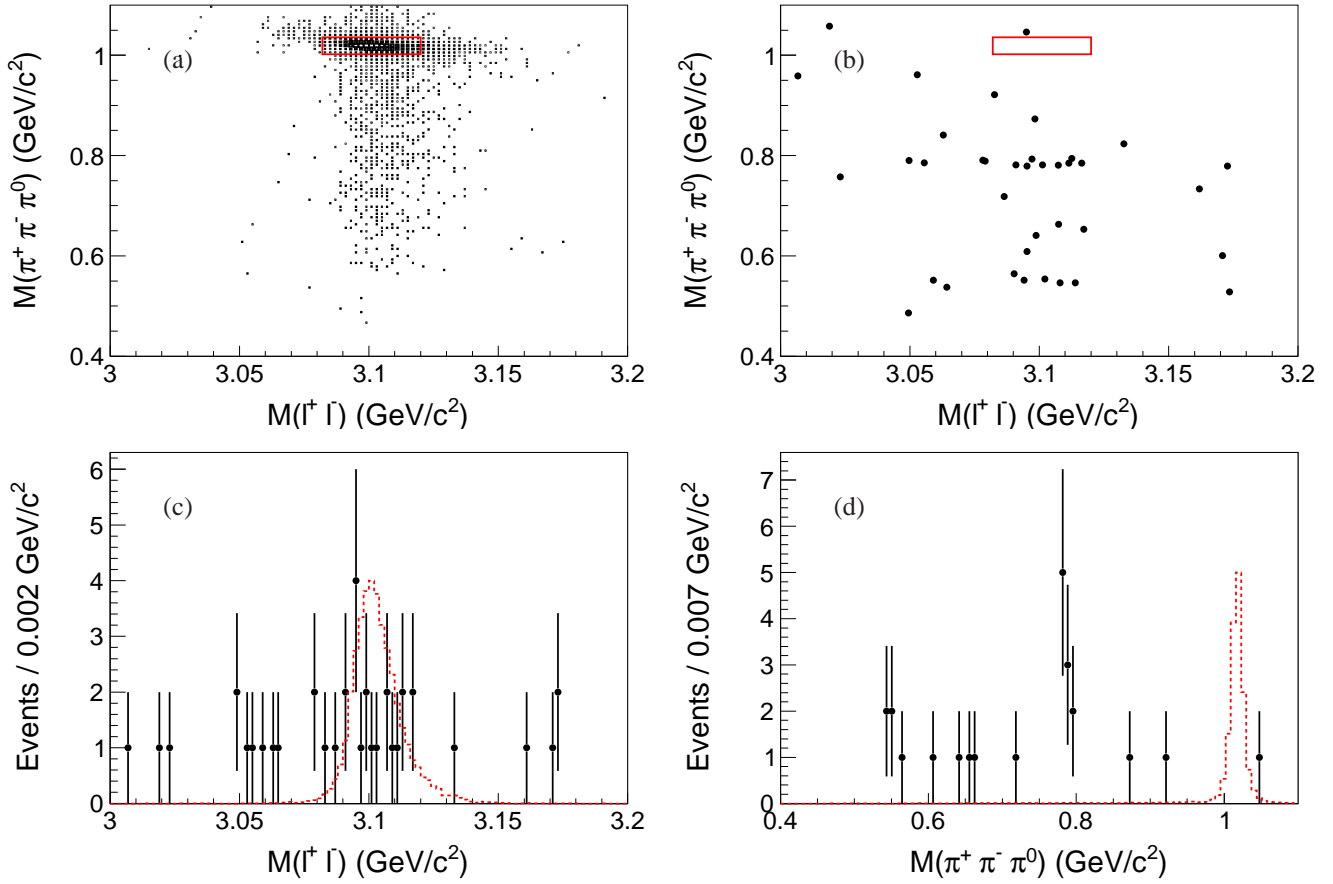


FIG. 5. Scatter plots for (a) signal MC, (b) data at 4.26 GeV, and the projections along (c) $M(\ell^+\ell^-)$ and (d) $M(\pi^+\pi^-\pi^0)$. The red box shows the applied mass windows of ϕ and J/ψ . The red dashed histogram shows the MC simulated shape (with arbitrary normalization).

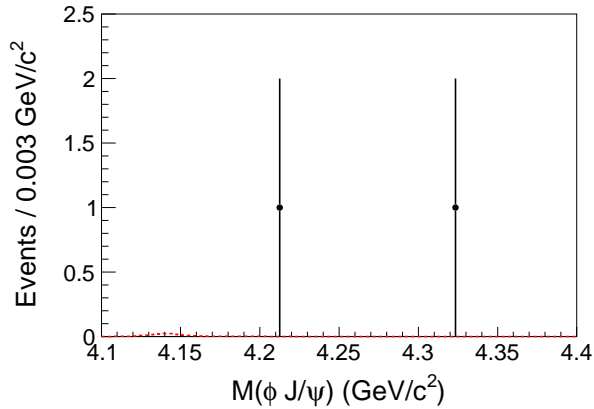


FIG. 6. Distribution of $M(\phi J/\psi)$ with $\phi \rightarrow \pi^+\pi^-\pi^0$ at $\sqrt{s} = 4.36$ GeV. The red dashed histogram represents the signal MC events scaled to the measured upper limit.

conservative. For the K_S^0 reconstruction, the difference between data and MC simulation is estimated to be 4.0% including tracking efficiencies for two daughter pions from the study of $J/\psi \rightarrow K^*\bar{K}^0 + c.c.$ [37].

The branching fractions for $\phi \rightarrow K^+K^-$, $K_S^0K_L^0$ and $\pi^+\pi^-\pi^0$, and $J/\psi \rightarrow e^+e^-$ and $\mu^+\mu^-$ are taken from the PDG [22]. The uncertainties of the branching fractions are taken as systematic uncertainties, which are 1.2%, 1.3%, and 2.2% for the process with $\phi \rightarrow K^+K^-$, $K_S^0K_L^0$, and $\pi^+\pi^-\pi^0$, respectively.

The radiative correction factor and detection efficiency are determined under the assumption that the production $e^+e^- \rightarrow \gamma Y(4140)$ follows the $Y(4260)$ line shape. The $Y(4360)$ line shape [22] is used as an alternative assumption, and the difference in $\epsilon \cdot (1 + \delta)$ is taken as a systematic uncertainty. This is 3.3%, 3.8%, and 10.0% for $\sqrt{s} = 4.23, 4.26$, and 4.36 GeV, respectively; the value for $\sqrt{s} = 4.36$ GeV is larger than others, since the line shape changes the biggest at this energy point.

The J^P of the $Y(4140)$ is unknown, and the efficiency is obtained from a MC sample generated uniformly in phase space. In order to estimate the uncertainty due to decay dynamics, the angular distribution of the radiative photon is generated as $1 + \cos^2 \theta$ and $1 - \cos^2 \theta$ to determine the difference of efficiency from that of the phase space MC sample. We take the biggest difference as the systematic uncertainty of the ra-

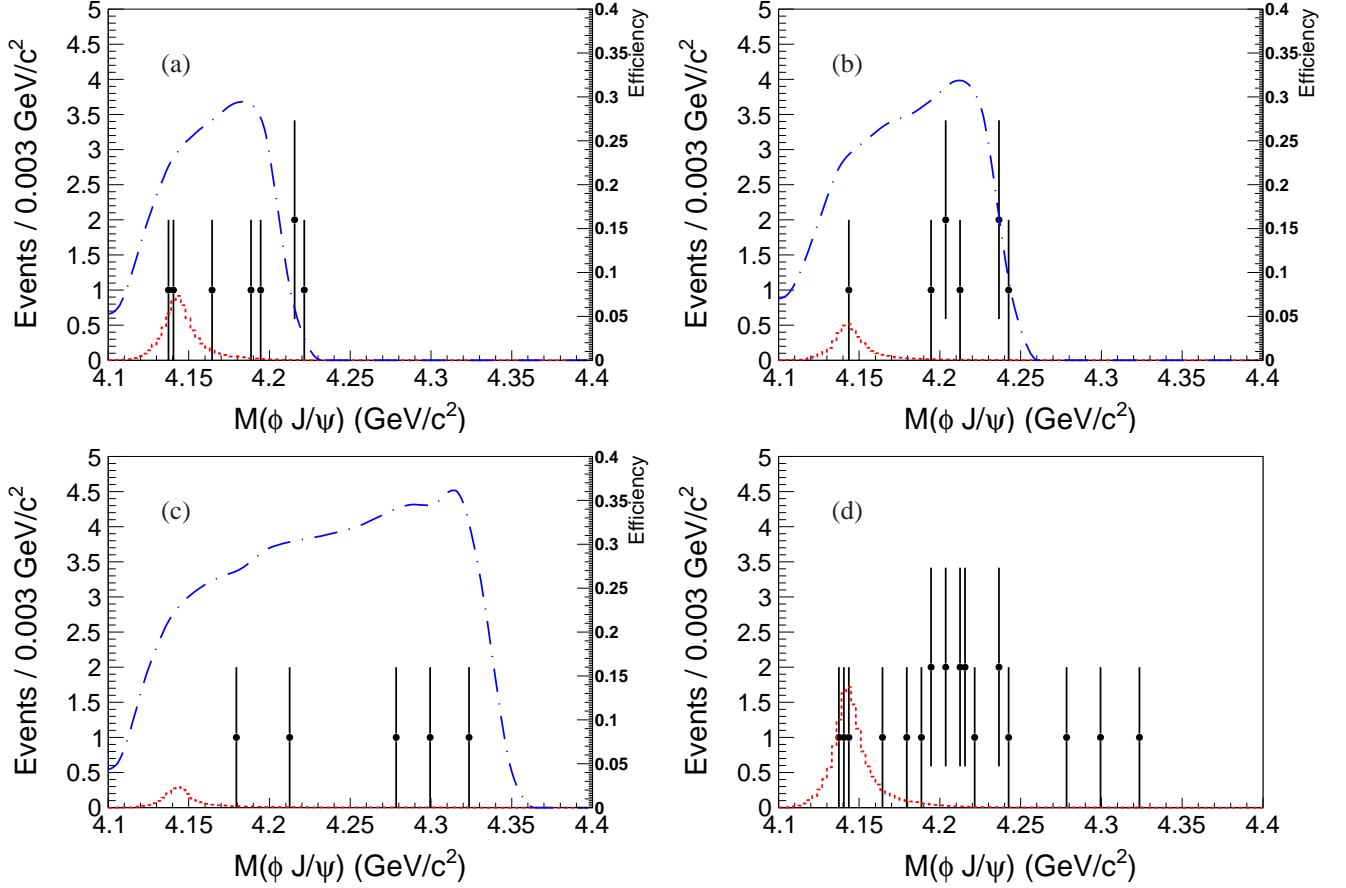


FIG. 7. Distribution of $M(\phi J/\psi)$ summed over all ϕ and J/ψ decay modes at $\sqrt{s} =$ (a) 4.23, (b) 4.26, (c) 4.36 GeV, and (d) the sum of three data samples. The red dashed histogram represents signal MC events scaled to our measured upper limit. The blue dashed-dot line shows the efficiency distribution.

diative decay distribution, which is 11.5%, 8.8%, and 13.5% for the modes $\phi \rightarrow K^+K^-$, $K_S^0 K_L^0$, and $\pi^+\pi^-\pi^0$, respectively.

For the J/ψ , ϕ , K_S^0 and π^0 mass windows, the selection is very loose, so the difference between data and MC simulation samples are negligible.

For the uncertainties due to kinematic fitting and vertex fitting, it is hard to find an appropriate control sample to measure them. A correction to the track helix parameters in the MC simulation [38] was applied so that the distribution of the MC simulation events is similar to that of the data, and we take half of the difference between the efficiency with and without this correction as the systematic uncertainty. The MC sample with the track helix parameter correction applied is used as the default in this analysis.

Assuming that all sources of systematic uncertainties are independent, the total errors are given by the quadratic sums of all of the above. At 4.26 GeV, the values, which are listed in Table III, are 13.2%, 12.5%, and 15.4%, for the modes $\phi \rightarrow K^+K^-$, $K_S^0 K_L^0$, and $\pi^+\pi^-\pi^0$, respectively. For the

events collected at 4.23 and 4.36 GeV, the only difference is the systematic uncertainty due to $(1 + \delta)$, and the total systematic errors are 13.1%, 12.4%, and 15.3% for events at 4.23 GeV, and 16.1%, 15.4%, and 17.9%, for events at 4.36 GeV.

VI. RESULTS AND DISCUSSIONS

In summary, we search for the $Y(4140)$ via $e^+e^- \rightarrow \gamma\phi J/\psi$ at $\sqrt{s} = 4.23, 4.26,$ and 4.36 GeV and observe no significant $Y(4140)$ signal in either data sample. The upper limits of the product of cross section and branching fraction $\sigma[e^+e^- \rightarrow \gamma Y(4140)] \cdot \mathcal{B}(Y(4140) \rightarrow \phi J/\psi)$ at the 90% C.L. are estimated as 0.35, 0.28, and 0.33 pb at $\sqrt{s} = 4.23, 4.26,$ and 4.36 GeV, respectively.

These upper limits can be compared with the $X(3872)$ production rates [34], which were measured with the same data samples by BESIII. The latter are $\sigma[e^+e^- \rightarrow \gamma X(3872)] \cdot \mathcal{B}(X(3872) \rightarrow \pi^+\pi^- J/\psi) = [0.27 \pm 0.09(\text{stat}) \pm$

0.02(syst)] pb, $[0.33 \pm 0.12(\text{stat}) \pm 0.02(\text{syst})]$ pb, and $[0.11 \pm 0.09(\text{stat}) \pm 0.01(\text{syst})]$ pb at $\sqrt{s} = 4.23, 4.26,$ and 4.36 GeV, respectively, which are of the same order of magnitude as the upper limits of $\sigma[e^+e^- \rightarrow \gamma Y(4140)] \cdot \mathcal{B}(Y(4140) \rightarrow \phi J/\psi)$ at the same energy.

The branching fraction $\mathcal{B}(Y(4140) \rightarrow \phi J/\psi)$ has not previously been measured. Using the partial width of $Y(4140) \rightarrow \phi J/\psi$ calculated under the molecule hypothesis [11], and the total width of the $Y(4140)$ measured by CDF [2], the branching fraction is estimated roughly to be 30%. A rough estimation for $\mathcal{B}(X(3872) \rightarrow \pi^+ \pi^- J/\psi)$ is 5% [39]. Combining these numbers, we estimate the ratio $\sigma[e^+e^- \rightarrow \gamma Y(4140)]/\sigma[e^+e^- \rightarrow \gamma X(3872)]$ is at the order of 0.1 or even smaller at $\sqrt{s} = 4.23$ and 4.26 GeV.

ACKNOWLEDGMENTS

The BESIII collaboration thanks the staff of BEPCII and the IHEP computing center for their strong support. This work is supported in part by National Key Basic Research Program

of China under Contract No. 2015CB856700; Joint Funds of the National Natural Science Foundation of China under Contracts Nos. 11079008, 11179007, U1232201, U1332201; National Natural Science Foundation of China (NSFC) under Contracts Nos. 10935007, 11121092, 11125525, 11235011, 11322544, 11335008; the Chinese Academy of Sciences (CAS) Large-Scale Scientific Facility Program; CAS under Contracts Nos. KJCX2-YW-N29, KJCX2-YW-N45; 100 Talents Program of CAS; INPAC and Shanghai Key Laboratory for Particle Physics and Cosmology; German Research Foundation DFG under Contract No. Collaborative Research Center CRC-1044; Istituto Nazionale di Fisica Nucleare, Italy; Ministry of Development of Turkey under Contract No. DPT2006K-120470; Russian Foundation for Basic Research under Contract No. 14-07-91152; U.S. Department of Energy under Contracts Nos. DE-FG02-04ER41291, DE-FG02-05ER41374, DE-FG02-94ER40823, DESC0010118; U.S. National Science Foundation; University of Groningen (RuG) and the Helmholtzzentrum fuer Schwerionenforschung GmbH (GSI), Darmstadt; WCU Program of National Research Foundation of Korea under Contract No. R32-2008-000-10155-0.

-
- [1] T. Aaltonen *et al.* (CDF Collaboration), *Phys. Rev. Lett.* **102**, 242002 (2009).
- [2] T. Aaltonen *et al.* (CDF Collaboration), arXiv: 1101.6058.
- [3] C. P. Shen *et al.* (Belle Collaboration), *Phys. Rev. Lett.* **104**, 112004 (2010).
- [4] R. Aaij *et al.* (LHCb Collaboration), *Phys. Rev. D* **85**, 091103 (2012).
- [5] S. Chatrchyan *et al.* (CMS Collaboration), *Phys. Lett. B* **734**, 261 (2014).
- [6] V. M. Abazov *et al.* (D0 Collaboration), *Phys. Rev. D* **89**, 012004 (2014).
- [7] J. P. Lees *et al.* (BABAR Collaboration), arXiv: 1407.7244.
- [8] X. Liu, *Phys. Lett. B* **680**, 137 (2009).
- [9] X. Liu and S. L. Zhu, *Phys. Rev. D* **80**, 017502 (2009).
- [10] N. Mahajan, *Phys. Lett. B* **679**, 228 (2009).
- [11] T. Branz, T. Gutsche, V. E. Lyubovitskij, *Phys. Rev. D* **80**, 054019 (2009).
- [12] M. E. Bracco *et al.*, *Nucl. Phys. B* **19**, 236 (2010).
- [13] G. J. Ding, *Eur. Phys. J. C* **64**, 297 (2009).
- [14] J. R. Zhang and M. Q. Huang, *Commun. Theor. Phys.* **54**, 1075 (2010).
- [15] F. Stancu, *J. Phys. G* **37**, 075017 (2010).
- [16] K. Yi, *Int. J. Mod. Phys. A* **28**, 1330020 (2013).
- [17] M. Ablikim *et al.* (BESIII Collaboration), *Nucl. Instrum. Methods Phys. Res., Sect. A* **614**, 345 (2010).
- [18] M. Ablikim *et al.* (BESIII Collaboration), *Phys. Rev. Lett.* **111**, 242001 (2013).
- [19] S. Agostinelli *et al.* (GEANT4 Collaboration), *Nucl. Instrum. Methods A* **506**, 250 (2003).
- [20] Z. Y. Deng *et al.*, *HEP & NP* **30**, 371 (2006).
- [21] S. Jadach, B. F. L. Ward and Z. Was, *Comput. Phys. Commun.* **130**, 260 (2000); *Phys. Rev. D* **63**, 113009 (2001).
- [22] K. A. Olive *et al.* (Particle Data Group), *Chin. Phys. C* **38**, 090001 (2014).
- [23] E. Barberio and Z. Was, *Comput. Phys. Commun.* **79**, 291 (1994).
- [24] D. J. Lange, *Nucl. Instrum. Methods A* **462**, 152 (2001).
- [25] R. G. Ping *et al.*, *Chinese Phys. C* **32**, 599 (2008).
- [26] T. Sjöstrand *et al.*, arXiv: hep-ph/0108264.
- [27] C. P. Shen *et al.*, (Belle Collaboration), *Phys. Rev. D* **89**, 072015 (2014).
- [28] B. Aubert *et al.*, (BABAR Collaboration), *Phys. Rev. D* **86**, 012008 (2012).
- [29] B. Aubert *et al.*, (BABAR Collaboration), *Phys. Rev. D* **76**, 092005 (2007).
- [30] X. L. Wang *et al.*, (Belle Collaboration), *Phys. Rev. D* **87**, 051101 (2013).
- [31] T. E. Coan *et al.*, (CLEO Collaboration), *Phys. Rev. Lett.* **96**, 162003 (2006).
- [32] E. A. Kuraev and V. S. Fadin, *Yad. Fiz.* **41**, 733-742 (1985).
- [33] F. Jegerlehner, arXiv: 1107.4683.
- [34] M. Ablikim *et al.* (BESIII Collaboration), *Phys. Rev. Lett.* **112**, 092001 (2014).
- [35] M. Ablikim *et al.* (BESIII Collaboration), *Phys. Rev. Lett.* **112**, 022001 (2014).
- [36] M. Ablikim *et al.* (BESIII Collaboration), *Phys. Rev. D* **81**, 052005 (2010).
- [37] M. Ablikim *et al.* (BESIII Collaboration), *Phys. Rev. D* **87**, 052005 (2013).
- [38] M. Ablikim *et al.* (BESIII Collaboration), *Phys. Rev. D* **87**, 012002 (2013).
- [39] C. Z. Yuan (for the Belle Collaboration), arXiv: 0910.3138. Proceedings of the XXIX PHYSICS IN COLLISION.